Metallophysics and Advanced Technologies
Металофіз. новітні технол.
Metallofiz. Noveishie Tekhnol.
2024, vol. 46, No. 8, pp. 755–769
https://doi.org/10.15407/mfint.46.08.0755
Reprints available directly from the publisher

PACS numbers: 68.47.Gh, 68.55.J-, 81.15.Cd, 81.40.-z, 81.65.Kn, 82.45.Bb, 87.85.jj

The Effect of Silver Coating on the Corrosion Behaviour of Ag-Doped Magnesium Alloy NZ30K in Ringer–Locke Solution

V. L. Greshta[*], O. E. Narivskyi[**], A. V. Dzhus[*], R. V. Ivashkiv[***], O. S. Kuprin[****]

[*]*Zaporizhzhia Polytechnic National University,*
64 Zhukovs'ky Str.,
UA-69063 Zaporizhzhia, Ukraine
[**]*LLC 'Ukrspetsmash',*
7 Haharina Str.,
UA-71100 Berdiansk, Ukraine
[***]*Karpenko Physico-Mechanical Institute of the N.A.S. of Ukraine,*
5 Naukova Str.,
UA-79060 Lviv, Ukraine
[****]*National Scientific Centre 'Kharkiv Institute of Physics and Technology',*
1 Akademichna Str.,
UA-61108 Kharkiv, Ukraine

The paper investigates the effect of silver coating on the corrosion behaviour of magnesium alloy NZ30K alloyed with 0.09 wt.% Ag in Ringer–Locke solution. Samples of the alloy under study are plated with a silver layer of 200–300 nm and 500 nm thickness using the DC-magnetron sputtering system equipped with a circular silver source and target (of 50 mm in diameter) in a gas discharge. An unbalanced magnetron in a 600 mA DC mode at a voltage of 400 V is used. The silver coating at a constant magnetron power of 240 W and a bias voltage of 100 V is applied. The deposition time of a silver layer of 200–300 nm is of 5 minutes, and for 500 nm, is of 15 minutes. As found, the steady-state value of the corrosion potential E_{cor} for the samples of the studied alloy clad with a silver layer of 200–300 nm is formed during 2060 s from –1.418 up to –1.4449 V, and with 500 nm layer, during 1880 s from –1.433 up to –1.465 V. As recorded, the steady-state value of E_{cor} for both samples is established in two stages. As found, the rate of shifting of the potential E_{cor}

Corresponding author: Victor Leonidovych Greshta
E-mail: greshtaviktor@gmail.com

Citation: V. L. Greshta, O. E. Narivskyi, A. V. Dzhus, R. V. Ivashkiv, and O. S. Kuprin, The Effect of Silver Coating on the Corrosion Behaviour of Ag-Doped Magnesium Alloy NZ30K in Ringer–Locke Solution, *Metallofiz. Noveishie Tekhnol.*, **46**, No. 8: 755–769 (2024). DOI: 10.15407/mfint.46.08.0755

for the studied samples in the negative direction at the first stage is of 0.062 and 0.034 mV/sec, respectively. As shown, the rate of shifting of E_{cor} in the negative direction for the sample with a coating thickness of 200–300 nm at this stage is by 1.82 times higher than for the sample with a coating thickness of 500 nm. This is due to a larger number of linear and point defects over the coating with a thickness of 200–300 nm than with 500 nm and more intense contact corrosion. During the transition from the first stage to the second one of the formation of the stationary value of the potential E_{cor}, its abrupt fluctuation of up to 5 mV is observed that is associated with the delamination of the coating from the alloy in the vicinity of corrosion pits on the surface of the samples due to the contact and crevice corrosions and the mechanical effect of hydrogen bubbles released at the cathodic areas (of silver coating). As shown, the steady-state value of the potential E_{cor} for the samples of the alloy under study with a coating thickness of 200–300 nm and 500 nm is more positive by 9 and 7%, respectively, than that of the sample of the same alloy without a silver layer. This proves that, by applying silver coatings with different thicknesses, it is possible to control the rate of corrosion dissolution of NZ30K alloy with Ag (0.09 wt.%) in Ringer–Locke solution, and this approach can be used for the fabrication of biodegradable implants for the treatment of broken human bones.

Key words: biodegradable implants, magnesium alloy for implants, silver coating on the surface of magnesium implants, local corrosion of magnesium implants clad with a silver layer.

У статті досліджено вплив покриття зі срібла на корозійну поведінку магнійового стопу NZ30K, леґованого 0,09 мас.% Арґентуму в розчині Рінґера–Локка. Зразки з досліджуваного стопу плакували шаром срібла товщиною у 200–300 нм і 500 нм, застосовуючи систему магнетронного розпорошення постійного струму, обладнану круглим джерелом і мішенню із срібла (діяметром у 50 мм) у газовому розряді. Незбалансований магнетрон використовували в режимі постійного струму у 600 мА за напруги у 400 В. Покриття зі срібла наносили за постійної потужности магнетрона у 240 Вт і напруги зміщення у 100 В. Час осадження шару срібла у 200–300 нм складав 5 хвилин, а 500 нм — 15 хвилин. Встановлено, що стаціонарне значення потенціялу корозії E_{cor} зразків з досліджуваного стопу, плакованого шаром срібла у 200–300 нм, формувалося впродовж 2060 сек від –1,418 до –1,4449 В, а з 500 нм — 1880 сек від –1,433 до –1,465 В. Зафіксовано, що стаціонарне значення E_{cor} обох зразків встановлювалося у два етапи. Виявлено, що швидкість зсування потенціялу E_{cor} досліджуваних зразків у більш від'ємний бік на першому етапі складала 0,062 і 0,034 мВ/сек відповідно. Показано, що швидкість зсування E_{cor} у більш від'ємний бік у зразку з товщиною покриття у 200–300 нм на цьому етапі була в 1,82 більше, ніж у зразку з покриттям товщиною у 500 нм. Це зумовлено більшою кількістю лінійних і точкових дефектів на покритті товщиною у 200–300, ніж у 500 нм, та інтенсивнішою контактною корозією. З переходом від першого до другого етапу формування стаціонарного значення потенціялу E_{cor} спостережено його стрибкоподібну флюктуацію до 5 мВ, що пов'язано з відшаруванням покриття від стопу в околі корозійних виразок на поверхні зразків внаслідок контактної та щілинної ко-

розій і механічного впливу бульбашок із водню, який виділявся на катодних ділянках (покриття зі срібла). Показано, що стаціонарне значення потенціялу E_{cor} зразків з досліджуваного стопу з товщиною покриття у 200–300 та 500 нм на 9 і 7% відповідно є більш позитивним, ніж у зразку з такого ж стопу, не плакованого шаром срібла. Це переконує, що, застосовуючи покриття зі срібла з різною товщиною, можна керувати швидкістю корозійного розчинення стопу NZ30K, леґованого Ag (0,09 мас.%) у розчині Рінґера–Локка, а такий підхід можна застосовувати для виробництва біорозкладних імплантатів для лікування зламаних кісток людей.

Ключові слова: біорозкладні імплантати, магнійовий стоп для імплантатів, покриття зі срібла на поверхні магнійових імплантатів, локальна корозія магнійових імплантатів, плакованих шаром срібла.

(Received 5 December, 2023; in final version, 11 March, 2024)

1. INTRODUCTION

Today, stainless steels, cobalt-containing and titanium alloys are most commonly used in the manufacture of bone fixation implants [1]. These materials can withstand mechanical loads throughout the duration of a person's treatment, but they can contribute to surgical complications, such as metal allergies, infections, or soft tissue necrosis in their vicinity [2]. At the same time, there is a need for surgical removal of implants after fusion of broken bones, which is a problem for paediatric patients [3] and increases medical costs [4]. Biodegradable implants made of polymers [5] and magnesium alloys [6–8] do not have these disadvantages. At the same time, polymeric materials have low mechanical characteristics, which limit their use [5]. However, magnesium alloys have an elastic modulus of 40 GPa, which is close to that of tubular bones [9], which contributes to the uniform redistribution of stresses during human treatment [10]. In addition, the yield strength of magnesium alloys [11] is higher than that of human bones (about 120 MPa) [12] and guarantees their reliable fixation during treatment. For biodegradable implants, aluminium-containing [13–16] and aluminium-free magnesium alloys based on Mg–Mn, Mg–Mn–Zn, Mg–Y–Zn and McGaw [17] systems are used, which meet the requirements for biodegradable implants in terms of mechanical characteristics. However, aluminium-alloyed magnesium alloys should be used with caution in implant production, as they can contribute to biological complications such as Alzheimer's disease, muscle breakdown, and reduced osteoclast activity [18–20]. The magnesium alloy NZ30K alloyed with Zn, Zr and Nd has no such reservations, and its additional alloying with silver made it possible to improve its mechanical characteristics [21], provide slow uniform corrosion dissolution in the Ringer–Locke solution [21] and antibacterial properties of the medium typical of antibiotics [22]. It is known that the rate of corro-

sion dissolution of magnesium alloys can also be controlled by strengthening its structure [23–25] or by applying various coatings [26]. Taking into account the above-mentioned information, the effect of silver coating on the corrosion behaviour of silver-alloyed NZ30K alloy in Ringer–Locke solution is investigated in this paper.

2. EXPERIMENTAL/THEORETICAL DETAILS

We studied samples of magnesium alloy NZ30K alloyed with silver (0.09 wt.%) smelted in an induction crucible furnace and subjected to aging [21]. The diameter of the samples was 12 and the length was 30 mm. Their chemical composition by XRD using the INKA ENERGY 350 has been determined (Table 1).

The samples of the alloy under study were clad with a layer of silver 200–300 and 500 nm thick using a DC-magnetron sputtering system equipped with a circular source and a target made of Ag (50 mm in diameter) in a gas discharge. The vacuum chamber of the system was a cylinder with an internal diameter and height of 500 mm. Cylindrical samples made of silver-alloyed NZ30K (Table 1) were chemically degreased and cleaned by ultrasonication in a hot ethanol bath for 10 minutes and dried in warm air. Then, they were mounted on a rotating (9 Hz) fixture located 90 mm from the sputtering source. Before the silver coating was deposited, air was pumped out of the chamber by a diffusion oil pump to a residual pressure of $1 \cdot 10^{-3}$ Pa. The samples were ion-etched at a bias potential of 1000 V for 15 minutes at a pressure of 1.5 Pa. An unbalanced magnetron in a 600 mA DC mode at 400 V has been used. The silver coating at a constant magnetron power of 240 W and a substrate bias voltage of 100 V has been applied. The argon pressure in the deposition chamber was 1.0 Pa. The time of silver deposition on the surface of the studied magnesium alloy was of 5 minutes for a coating thickness of 200–300 nm and of 15 minutes for 500 nm.

Corrosion tests of silver clad samples have been carried out in a Ringer–Locke solution (an aqueous solution of undissociated water with the following chemical reagents, in mg/l: NaCl—9, $NaHCO_3$, $CaCl_3$, KCl—0.2, CHO_{6126}—1 at a temperature of 20 ± 1°C.

The establishment of a stationary value of the corrosion potential E_{cor} on the tested samples on the PN-2MK-10A potentiostat in automatic mode has been recorded. The surface of corrosion damage on the

TABLE 1. Chemical composition of silver alloy NZ30K.

Alloy		Content of chemical elements, wt.%			
NZ30K+Ag	Mg	Zn	Zr	Nd	Ag
	95.57	0.69	0.86	2.76	0.09

samples after their testing in the Ringer–Locke solution using an optical microscope MMR-2P has been examined.

3. RESULTS AND DISCUSSION

According to the results of corrosion tests of a sample made of NZ30K alloy additionally alloyed with Ag and clad with a silver layer 200–300 nm thick, it has been found that its potential E_{cor} intensively shifted to the negative side from –1.41776 and –1.41904 at points 1, 2 up to –1.4408 and –1.44048 at points 18, 19 (Table 2) during its exposure to the test solution for the first 384 seconds of testing.

After further exposure of the sample in the test solution for 1684 seconds, the establishment of a stationary value of the potential E_{cor} has been observed (Fig. 1).

It varied in a narrow interval from –1.4420 at point No. 20 up to –1.4448, –1.4442, –1.4448 and –1.4432 at points Nos. 60, 78, 79 and

TABLE 2. Corrosion potentials E_{cor} of NZ30K alloy additionally alloyed with Ag and clad with a layer of silver 200–300 nm thick depending on the time (τ) of exposure of samples in Ringer–Locke solution.

No. of points	τ, s	E_{cor}, V	No. of points	τ, s	E_{cor}, V	No. of points	τ, s	E_{cor}, V	No. of points	τ, s	E_{cor}, V
1	4	–1,41776	**21**	500	–1,44	**41**	1000	–1,44192	**61**	1520	–1,44288
2	24	–1,41904	**22**	520	–1,43872	**42**	1020	–1,4416	**62**	1540	–1,44384
3	44	–1,42064	**23**	540	–1,44064	**43**	1060	–1,4432	**63**	1580	–1,4432
4	64	–1,4232	**24**	560	–1,43968	**44**	1080	–1,44224	**64**	1600	–1,44352
5	84	–1,42384	**25**	580	–1,43904	**45**	1100	–1,4432	**65**	1660	–1,4432
6	104	–1,42672	**26**	600	–1,44128	**46**	1140	–1,44224	**66**	1680	–1,44448
7	124	–1,4264	**27**	640	–1,43904	**47**	1160	–1,4432	**67**	1700	–1,44256
8	144	–1,42864	**28**	660	–1,44192	**48**	1180	–1,4432	**68**	1740	–1,44352
9	164	–1,42864	**29**	680	–1,44192	**49**	1220	–1,44288	**69**	1760	–1,44288
10	184	–1,4312	**30**	700	–1,44064	**50**	1240	–1,44224	**70**	1780	–1,44192
11	204	–1,4312	**31**	720	–1,44064	**51**	1260	–1,44288	**71**	1800	–1,4432
12	224	–1,43344	**32**	760	–1,44064	**52**	1300	–1,44256	**72**	1840	–1,4432
13	244	–1,4344	**33**	780	–1,44224	**53**	1320	–1,44288	**73**	1860	–1,44384
14	264	–1,436	**34**	800	–1,4416	**54**	1340	–1,4432	**74**	1900	–1,44384
15	284	–1,436	**35**	820	–1,4416	**55**	1360	–1,4432	**75**	1920	–1,44352
16	304	–1,43632	**36**	840	–1,44192	**56**	1400	–1,44256	**76**	1980	–1,44288
17	324	–1,43792	**37**	860	–1,44256	**57**	1420	–1,44352	**77**	2000	–1,4432
18	344	–1,4408	**38**	900	–1,44224	**58**	1440	–1,44352	**78**	2040	–1,44416
19	364	–1,44048	**39**	940	–1,44256	**59**	1460	–1,44384	**79**	2060	–1,4448
20	384	–1,44208	**40**	980	–1,44288	**60**	1480	–1,4448	**80**	2068	–1,4432

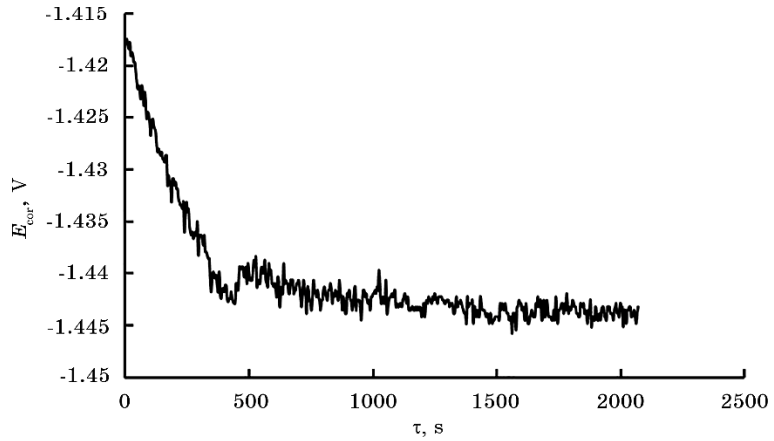

Fig. 1. Dependence between the corrosion potential E_{cor} of NZ30K alloy additionally alloyed with Ag and clad with a silver layer of 200–300 nm thickness on the time of exposure of samples (τ) in Ringer–Locke solution.

80, respectively (Table 2). It has been found that the incubation period for the formation of a stationary value of the corrosion potential E_{cor} on the sample clad with a silver layer of 200–300 nm thick was of about 400 seconds after its immersion in the Ringer–Locke solution (Table 2). During this interval, the potential E_{cor} shifted to the negative side at a rate of 0.062 mV/s (Fig. 1), which is 1.22 times more intense than the shift to the positive side on the sample made of NZ30K alloy additionally alloyed with Ag and not clad with a silver layer [27]. Corrosion studies have shown that even a very small thickness of the silver layer on the surface of the alloy under study contributes to a shift in its potential E_{cor} to the positive side by about 0.06 V. This is because the standard potential of magnesium in a solution of its own salts is of –2.36, and that of silver is of +0.8 V [28]. With a perfectly dense silver coating on a magnesium alloy, the sample potential would be close to the value of the standard potential of silver in a solution of its salts. However, the results of corrosion studies have shown that the potential E_{cor} of a sample coated with a silver layer 200–300 nm thick is positive not much more than that of an uncoated sample of NZ30K alloy additionally alloyed with Ag [27]. This is because the coating on the surface of the alloy under study has a small thickness and defects (Fig. 2).

In particular, point defects up to 1 μm in size and linear macrostratification on the surface of the clad silver layer with a thickness of 200–300 nm have been found, which contributed to the contact of the alloy under study with the Ringer–Locke solution, where galvanic pairs with a high potential difference (of about 3 V) have been formed. Intensive contact corrosion of the alloy in these areas has been observed,

Fig. 2. Point and linear defects of the clad silver layer with a thickness of 200–300 nm on the surface of NZ30K alloy additionally doped with Ag (×800).

as it has a much more negative potential value than silver. The consequences of contact and subsequently crevice corrosion of the sample surface are shown in Fig. 3.

It revealed large corrosion ulcers up to 1000 μm in size formed because of anodic dissolution of metals from the alloy and small corrosion damage up to 2 μm in the silver clad layer, which most likely originated in places of its minimum thickness at the tops of the alloy microrelief (Fig. 3). Using the Image J computer program, it has been found that the total area of localized corrosion damage on the end surface of the sample was 13.26 mm^2. This is 26.4% of the total area of the sample and 1.63 times larger than that of a sample of the same alloy not clad with silver [27]. It is known [29, 30] that in chloride-containing media, which is also a Ringer–Locke solution, steels and alloys are subject to pitting corrosion. At the same time, the more pitting on their surface, the lower the rate of their growth due to the redistribution of anode current density between a larger number of them [31]. The analysis of local corrosion damage on the surface of the samples showed that the number, area, and depth of pittings on the samples coated with a silver layer with a thickness of 200–300 nm (Fig. 3) are greater than on the uncoated samples [27]. This is due to the fact that the uncoated alloy underwent pitting and ulcer corrosion by the mechanisms inherent in

Fig. 3. The surface of NZ30K alloy additionally alloyed with Ag and clad with a layer of silver 200–300 nm thick after corrosion tests in Ringer–Locke solution.

pitting corrosion [30]. However, a sample of the same alloy clad with a silver layer 200–300 nm thick underwent corrosion pitting, mainly due to the mechanisms of contact corrosion, which is characterized by the potential difference between the materials of the contact pairs [32].

A characteristic feature of both mechanisms of local corrosion of samples is the selective dissolution of metals from the surface of corrosion damage. This is consistent with well-known data from [30, 33] and may contribute to the enrichment of anodic areas on the surface of samples with chemical elements that are capable of forming stable oxide films resistant to local corrosion in the chlorine ion media. In stainless steels and alloys, such a component is chromium [34–37], and in the studied NZ30K + Ag alloy, it is Zr, Zn, and Nd. At the same time, due to the redistribution of currents between a large number of corrosion damage on the surface of the sample, as mentioned above [31], conditions can be created for their repassivation through the formation of Zr-, Zn-, and Nd-containing oxide films on their surface and a decrease in the potential difference between the coating and the alloy in the process of its corrosion–mechanical destruction.

Summarizing the above-mentioned information, it can be noted that the rate of local corrosion of the sample clad with a silver layer with a thickness of 200–300 nm is higher than that of the uncoated sample, which is due to different mechanisms of these processes. It should be noted that local corrosion processes on both samples occurred mainly during the establishment of the stationary value of E_{cor}, and then, local corrosion turned into general corrosion, which meets the requirements

Fig. 4. Point defects of a 500 nm thick silver clad layer on the surface of NZ30K + Ag alloy (×500).

for biodegradable implants. At the same time, they need to have an optimal dissolution rate in the human body [39], similar elastic modulus values to tubular bones [36] for satisfactory stress redistribution [40], and yield strength not less than that of bones for reliable fixation for the entire treatment period [41–43]. The NZ30K + Ag alloy meets these requirements, as its yield strength is 137 MPa [44] and that of tubular bone is 120 MPa [42], it is non-toxic, does not contribute to metal allergy, infections and soft tissue necrosis in the vicinity of implants [2, 18–20], and selectively dissolved Ag ions can be a source of disinfection of human soft tissue [45]. Taking into account the above-mentioned data and the information of Ref. [38], the NZ30K + Ag alloy clad with a silver layer of 200–300 nm thickness can be recommended for the production of biodegradable implants after positive clinical trials. To optimize the rate of their decomposition, samples of this alloy clad with 500 nm silver layer have been studied. Metallographic analysis revealed that the sample surface contained only point defects of up to 0.5 μm (Fig. 4).

This significantly affects the dynamics of establishing the stationary value of the corrosion potential E_{cor} of the sample during its study in the Ringer–Locke solution (Fig. 5).

In particular, the results of the analysis of the dependence E_{cor}–τ (Fig. 5) showed that it was formed in two stages. At the first stage, during 104 seconds after the sample was immersed in the test solution, the following values of the potentials E_{cor} have been recorded: –1.43324, –1.43452, –1.43484, –1.43612, –1.43708 at points 1–5, respectively (Table 3). However, after 500 and 524 seconds of corrosion testing, they are linearly shifted in the negative direction to –1.45404,

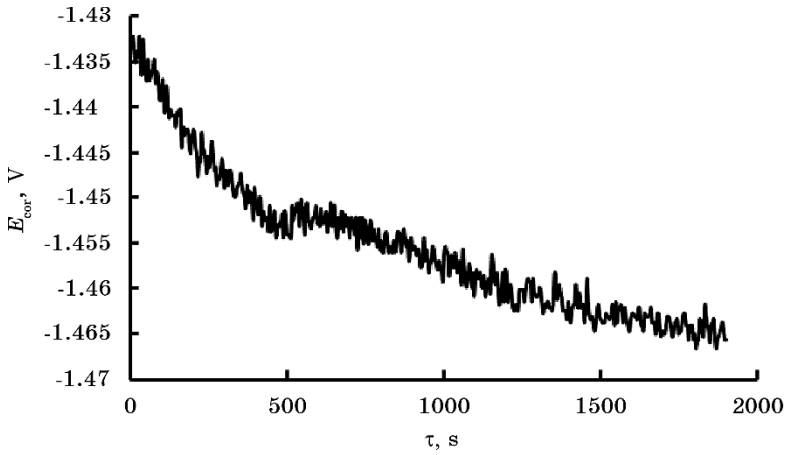

Fig. 5. Dependence of the corrosion potential E_{cor} of NZ30K alloy additionally alloyed with Ag and clad with a 500 nm thick silver layer on the exposure time (τ) of the sample in Ringer–Locke solution.

–1.45512 V (see points 21, 22, respectively, in Table 3).

It should be noted that at this stage of the corrosion tests, the rate of shift of the potential E_{cor} in the negative direction was of 0.034 mV/s. This is 1.82 times slower than for the sample with a coating thickness of 200–300 nm (Figs. 1, 5), which is due to slower contact corrosion of the sample plated with a 500 nm thick silver layer. This was facilitated by the smaller size of the pitting and the absence of linear defects on the surface of the 500 nm-thickness coating. It should be noted that, at the end of the first stage of formation of the stationary value of the corrosion potential E_{cor} on both samples (Figs. 1, 5), a slight shift of this potential to the positive side by 5 mV has been recorded. This is due to the local destruction of the coating on the surface of the tested samples under the influence of a stream of hydrogen bubbles formed on the cathodic areas, i.e. the surface of the silver coatings, which has been determined visually. Further, an intensive shift of the potential E_{cor} in the negative direction to –1.46144, –1.46496, –1.4656 V at points 48, 52, 71, 75 (Table 3), respectively, has been found. This tendency is inherent in the second stage of establishing the stationary value of E_{cor} during 1256 seconds of testing (from point 22 to point 75 in Table 3).

At this stage, a less intense corrosion–mechanical destruction of the coating was observed than at the first stage, since the potential E_{cor} of the sample shifted to the negative side at a rate of 0.01 mV/s (from point 22 to point 52 in Table 3) until the stationary value of –1.466 V has been established. It is associated with the stabilization of anodic–cathodic processes on the surface of the sample after corrosion–

TABLE 3. Corrosion potentials E_{cor} of NZ30K alloy additionally alloyed with Ag and clad with a 500 nm-thickness silver layer depending on the time (τ) of exposure of the sample to Ringer–Locke solution.

No. of points	τ, s	E_{cor}, V	No. of points	τ, s	E_{cor}, V	No. of points	τ, s	E_{cor}, V	No. of points	τ, s	E_{cor}, V
1	4	–1,43324	**21**	500	–1,45404	**41**	1000	–1,45632	**61**	1500	–1,46336
2	24	–1,43452	**22**	524	–1,4512	**42**	1020	–1,4576	**62**	1520	–1,46304
3	44	–1,43484	**23**	544	–1,45024	**43**	1060	–1,45568	**63**	1540	–1,46208
4	84	–1,43612	**24**	584	–1,45216	**44**	1080	–1,45728	**64**	1560	–1,46208
5	104	–1,43708	**25**	604	–1,45312	**45**	1100	–1,45888	**65**	1580	–1,46304
6	124	–1,44124	**26**	624	–1,45152	**46**	1120	–1,45984	**66**	1600	–1,46272
7	164	–1,44444	**27**	644	–1,45312	**47**	1140	–1,4592	**67**	1620	–1,46208
8	184	–1,44252	**28**	684	–1,45184	**48**	1180	–1,46144	**68**	1640	–1,46272
9	204	–1,44284	**29**	704	–1,45216	**49**	1200	–1,45856	**69**	1660	–1,46208
10	244	–1,44732	**30**	724	–1,45568	**50**	1220	–1,46208	**70**	1680	–1,46272
11	264	–1,44508	**31**	744	–1,45504	**51**	1260	–1,46016	**71**	1700	–1,46496
12	304	–1,447	**32**	784	–1,45472	**52**	1280	–1,46144	**72**	1720	–1,46336
13	324	–1,44796	**33**	804	–1,456	**53**	1300	–1,4608	**73**	1740	–1,46368
14	364	–1,44988	**34**	824	–1,456	**54**	1320	–1,46176	**74**	1760	–1,46336
15	384	–1,45052	**35**	844	–1,456	**55**	1360	–1,46112	**75**	1780	–1,4656
16	404	–1,45084	**36**	884	–1,45472	**56**	1380	–1,4624	**76**	1800	–1,46496
17	424	–1,45148	**37**	904	–1,45536	**57**	1400	–1,46304	**77**	1820	–1,46368
18	444	–1,45084	**38**	924	–1,4576	**58**	1420	–1,45952	**78**	1840	–1,464
19	464	–1,45436	**39**	944	–1,45568	**59**	1440	–1,46208	**79**	1860	–1,46336
20	484	–1,4518	**40**	984	–1,45696	**60**	1480	–1,46464	**80**	1880	–1,46464

mechanical destruction of the coating (Fig. 6).

An analysis of the surface of the 500 nm-thickness coated specimen after its corrosion tests in Ringer–Locke solution showed that it suffered the greatest localised corrosion damage at its ends, where the coating adhered to the alloy with the lowest adhesion (Fig. 6). In particular, on the right side of the sample (Fig. 6), the coating was detached from the alloy surface. This is obviously due to the local contact of the alloy with the Ringer–Locke solution and the formation of contact pairs between it and the coating. Under such conditions, anodic and cathodic processes were accelerated with the formation of hydrogen bubbles on the coating, which contributed to its detachment from the alloy and the formation of a gap between them, which was filled with the solution. This also contributed to the development of crevice corrosion on the sample.

It should be noted that the formation of a stationary value of the corrosion potentials E_{cor} of NZ30K and NZ30K + Ag alloys occurred

Fig. 6. The surface of NZ30K alloy additionally doped with Ag and clad with a 500 nm-thickness silver layer after corrosion tests in Ringer–Locke solution.

under the influence of selective dissolution of the most electronegative magnesium component from its surface, so their E_{cor} shifted to the positive side after immersion of the samples in the Ringer–Locke solution. However, the E_{cor} potentials of the NZ30K + Ag alloy samples clad with a silver layer of 200–300 nm- and 500 nm-thickness shifted to the negative side before its steady-state value has been established, which was due to pitting, contact, and crevice corrosions, which are formed and developed on point and linear coating defects. This one occurred in two stages. For a sample with a coating thickness of 500 nm, the first stage lasted about 400 s, and its potential E_{cor} shifted to the negative side at a rate of 0.034 mV/s, which is 1.82 times slower than for a sample with a coating thickness of 200–300 nm. The second stage for both types of samples was longer (up to 1500 s) and was characterized by corrosion–mechanical destruction of the coating and a very slow shifting of E_{cor} of the sample with a coating thickness of 200–300 nm in the negative direction (of about 2 mV during 1500 s) and slightly faster for the sample with a coating thickness of 500 nm (0.01 mV/s).

These corrosion–mechanical processes on the surface of the samples contributed to the fact that its E_{cor} potential was 95 (200–300 nm) and 75 mV (500 nm) more positive than that of a sample of the same alloy not plated with silver. This shows that these coatings on the surface of the NZ30K + Ag alloy can be used to control the dissolution rate and to disinfect additionally surgical sites with selectively dissolved silver from the alloy and coating.

4. CONCLUSIONS

According to the results of the research, it has been found that the corrosion potential E_{cor} of samples made of NZ30K alloy alloyed with Ag and clad with a silver layer of 200–300 nm- and 500 nm-thickness shifted in the negative direction from –1.418 up to –1.449 V during 2060 s and from –1.433 up to –1.465 V during 1880 s of exposure in the Ringer–Locke solution, respectively, until its stationary value has been established. During the first 400 seconds of testing the samples, the most intense shift of this potential to the negative side at a rate of 0.062 and 0.034 mV/s has been observed, respectively. The potential E_{cor} of the samples coated with a silver layer with a thickness of 200–300 nm was 1.82 times more intensively shifted to the negative side than that of the samples with a coating thickness of 500 nm. This is due to the more intense contact and crevice corrosion of the former on coating imperfections. Further, after 400 seconds of research, a jump-like fluctuation of E_{cor} has been detected, which is associated with the delamination of the coating from the alloy under the influence of crevice corrosion and the mechanical pressure of the flow of hydrogen bubbles on it, which was released at the cathode areas. After establishing the steady-state value of the potential E_{cor}, both samples showed mainly uniform corrosion dissolution at a rate by 1.09 and 1.07 times lower than that of the sample of the same alloy without coating, if take into account the steady-state values of their potentials E_{cor}. It has been shown that silver coating on NZ30K alloy additionally alloyed with silver (0.09 wt.%) can be used to control the rate of its corrosion dissolution in Ringer–Locke solution and recommend this approach for implant manufacturing.

REFERENCES

1. D. Gibbons, *ASM Handbook: Vol. 23: Materials for Medical Devices* (Ed. R. J. Narayan) (Materials Park, OH: ASM International: 2012), Ch. Introduction to Medical Implant Materials, p. 3.
2. B. D. Ratner, A. S. Haffman, F. J. Schoen, and J. E. Lemons, *An Introduction to Materials in Medicine. Third Edition* (Academic Press: 2013).
3. M. L. Busam, R. J. Ester, and W. T. Obremskey, *Journal of the American Academy of Orthopaedic Surgeons*, **14**, No. 2: 113 (2006).
4. M. P. Staiger, A. M. Pietak, J. Huadmai, and G. Dias, *Biomaterials*, **27**, No. 9: 1728 (2006).
5. A. Denkena and B. Lucas, *Biocompatible Magnesium Alloys as Absorbable Implant Materials – Adjusted Surface and Subsurface Properties by Machining Processes, CIRP Annals*, **56**, Iss. 1: 113 (2007).
6. M. Esmaily, J. E. Svensson, S. Fajardo, N. Birbilis, G. S. Frankel, S. Virtanen, R. Arrabal, S. Thomas, and L. G. Johansson, *Progr. Mater. Sci.*, **89**: 192–193 (2017).

7. G. L. Song and Z. Shi, *Corrosion Science*, **85**: 126 (2014).
8. A. D. King, N. Birbilis, and J. R. Scully, *Electrochimica Acta.*, **121**: 394 (2014).
9. S. C. Cowin, A. E. Goodship and J. L. Cunningham, *Bone Mechanics Handbook. Second Edition* (Boca Raton, FL: CRC Press: 2001), Ch. 5.
10. M. E. Müller, M. Allgöwer, R. Schneider and H. Willenegger, *Manual of Internal Fixation. Techniques Recommended by the AO Group* (Berlin–Heidelberg: Springer: 1991).
11. X.-N. Gu and Y.-F. Zheng, *Front. Mater. Sci. China*, **4**: 111 (2010).
12. Y. N. An and R. A. Draughn, *Mechanical Testing of Bone and the Bone-Implant Interface* (Boca Raton: CRC Press: 1999).
13. W. D. Müller, M. L. Nascimento, M. Zeddies, M. Cyrsico, L.M. Gassa, and M. A. F. L. D. Mele, *Materials Research*, **10**: 5 (2007).
14. F. Witte, H. Ulrich, M. Rudert, and E. Willbold, *Journal of Biomedical Materials Research. Part A*, **81**: 748 (2007).
15. L. Xu, G. Yu, E. Zhang, F. Pan, and K. Yang, *Journal of Biomedical Materials Research. Part A*, **83**, No. 3: 703 (2007).
16. G. D. Zhang, J. J. Huang, K. Yang, B. C. Zhang, and H. J. Ai, *Acta Metall. Sin.*, **43**: 1186 (2007).
17. H. E. Friedrich and B. L. Mordike, *Magnesium Technology*, **212**: 677 (2006).
18. P. C. Ferreira, K. D. A. Piai, A. M. M. Takayanagui, and S. I. Segura-Mucoz, *Rev. Latino-Am. Enfermagem*, **16**, No. 1: 151 (2008).
19. Y. Okazaki, S. Rao, Y. Ito, and T. Tateishi, *Biomaterials*, **19**, No. 13: 1197 (1998).
20. N. Cases, *The Medical Journal of Australia*, **183**, No. 3: 145 (2005).
21. V. Greshta, V. Shalomeev, A. Dzhus, and O. Mityaev, *Novi Materialy ta Tekhnolohiyi v Metalurgiyi ta Mashynobuduvanni* [New Materials and Technologies in Metallurgy and Mechanical Engineering], **2**: 14 (2023) (in Ukrainian).
22. M. F. Kulyk, T. V. Zasukha, and M. B. Lutsyuk, *Saponite and Aerosil in Animal Husbandry and Medicine* (Vinnytsia: FOP Rogalska I.O.: 2012).
23. T. C. Lowe and R. Z. Valiev, *Advanced Biomaterials and Biodevices* (2014), p. 1.
24. W. Xu, N. Birbilis, G. Sha, and Y. Wang, *Nature Mater.*, **14**, No. 12: 1229 (2015).
25. H. R. B. Rad, M. H. Idris, M. R. A. Kadir, and S. Farahan, *Materials & Design*, **33**: 88 (2012).
26. G. L. Makar and J. Kruger, *Inter. Mater. Rev.*, **38**, No. 3: 138 (1993).
27. V. L. Greshta, O. E. Narivskyi, A. V. Dzhus, and V. A. Vynar, *Phys. Sci. and Technol.*, **10**, No. 2 (2023).
28. H. Baker, *ASM Specialty Handbook: Magnesium and Magnesium Alloys* (Materials Park, OH: ASM International: 1999).
29. O. E. Narivs'kyi, *Fiz.-Khim. Mekh. Mater.*, **41**, No. 1: 104 (2005).
30. O. E. Narivs'kyi, *Mater. Sci.*, **43**, No. 1: 124 (2007).
31. O. E. Narivs'kyi, *Mater. Sci.*, **43**, No. 2: 256 (2007).
32. I. L. Rosenfel, *Korroziya i Zashchita Metallov* [Corrosion and Protection of Metals] (Moskva: Metallurgy: 1970) (in Russian).
33. N. V. Vyazovikina, *Ehlektrokhimiya*, **6**: 917 (1992) (in Russian).
34. O. E. Narivskyi, S. O. Subbotin, T. V. Pulina, S. O. Leoshchenko, M. S. Khoma, and N. B. Ratska, *Mater. Sci.*, **58**, No. 5: 1 (2023).

35. O. E. Narivskyi, S. A. Subbotin, T. V. Pulina, and M. S. Khoma, *Mater. Sci.*, **58**: 41 (2022).
36. O. E. Narivskyi, S. B. Belikov, S. A. Subbotin, and T. V. Pulina, *Mater. Sci.*, **57**, No. 2: 291 (2021).
37. O. Narivs'kyi, R. Atchibayev, A. Kemelzhanova, G. Yar-Mukhamedova, G. Snizhnoi, and S. Subbotin, *Eurasian Chemico-Technological Journal*, **24**, No. 4: 295 (2022).
38. F. Witte, V. Kaese, H. Haferkamp, E. Switzer, C. Meyer-Lindenberg, C. J. Wirth, and H. Windhagen, *Biomaterials*, **26**: 3557 (2005).
39. W.A. Badawy, N. H. Hilal, M. El-Rabee, and H. Nady, *Electrochimica Acta*, **55**, No. 6: 1880 (2010).
40. S. Abela, *Corrosion and Surface Treatments*, **10**: 195 (2011).
41. H. Hornberger, S. Virtanen, and A. R. Boccaccini, *Acta Biomaterialia*, **8**, No. 7: 2442 (2012).
42. K. Y. Chiu, M. H. Wong, F. T. Cheng, and H. C. Man, *Surface and Coatings Technology*, **202**, No. 3: 590 (2007).
43. M. Carboneras, M. C. García-Alonso, and M. L. Escudero, *Corrosion Science*, **53**, No. 4: 1433 (2011).
44. H. M. Wong, K. W. K. Yeung, K. O. Lam, V. Tam, P. K. Chu, K. D. K. Luk, and K. M. C. Cheung, *Biomaterials*, **31**, No. 8: 2084 (2010).
45. Z. Zhen, T. Xi, and Y. Zheng, *Transactions of Nonferrous Metals Society of China*, **23**, No. 8: 2283 (2013).